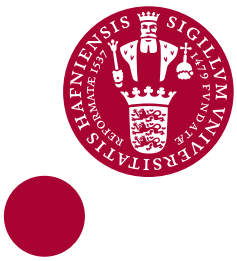

Conjugation Length Dependence of Free Radical Scavenging Efficiency of Retinal and Retinylisoflavonoid Homologues

Jiang, Yang-Lin; Chen, Bai-Ling; Yan, Xiao-Kun; Xu, Yi; Zhao, Chen-Chen; Chen, Zi-Li; Wang, Peng; Zhang, Jian-Ping; Skibsted, Leif H.

Published in:
ACS Omega

DOI:
10.1021/acsomega.0c00925

Publication date:
2020

Document version
Publisher's PDF, also known as Version of record

ACS OMEGA

http://pubs.acs.org/journal/acsodf

Article

Conjugation Length Dependence of Free Radical Scavenging Efficiency of Retinal and Retinylisoflavonoid Homologues

Yang-Lin Jiang, Bai-Ling Chen, Xiao-Kun Yan, Yi Xu, Chen-Chen Zhao, Zi-Li Chen, Peng Wang,* Jian-Ping Zhang, and Leif H. Skibsted

Cite This: *ACS Omega* 2020, 5, 13770−13776

Read Online

ACCESS | Metrics & More | Article Recommendations | Supporting Information

ABSTRACT: Retinal (C20) and the C25 and C30 homologues were compared as radical scavengers together with their C22, C27, and C32 homologues linked with daidzein through a B′3 (isoflavonoid) to oxo-carbon (aldehyde) covalent bond. Oxidation potential in acetonitrile determined by cyclic voltammetry and ionization potential calculated by density functional theory for the aldehydes and dyads (conjugates), of which the two longer are new, decreased linearly with the wavenumber for absorption maximum. The logarithm of the second-order rate constant for scavenging of the $ABTS^{\bullet+}$ increased linearly with decreasing oxidation potential suggesting that longer conjugation in the antioxidant increases the rate of electron transfer. A similar linear free energy relationship was found for the rate of scavenging $DPPH^{\bullet}$, including daidzein, which may indicate involvement of hydrogen atom transfer from an isoflavonoid phenol. Prediction of radical scavenging efficiency from visible absorption spectra was demonstrated with the perspective of rational design of bifunctional amphiphilic antioxidants.

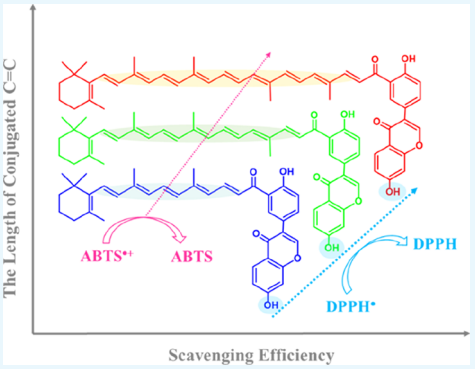

INTRODUCTION

Carotenoids are important for the stability of biological membranes under oxidative stress.[1,2] The antioxidant effect depends on electron donation to lipid and protein radicals, and the carotenoids with the longest linear conjugation of carbon double bonds are the most reducing and often the most efficient radical scavengers.[3,4] Other factors such as polarity and orientation in the membrane and interaction with other antioxidants are, however, also important for the protection of membranes by carotenoids.[1,5] Similar interaction between carotenoids and flavonoids has been observed during extraction of antioxidants from plant materials.[6−9] The interaction between carotenoids and plant phenols in the lipid−water interface has thus recently been found important for membrane integrity using giant unilamellar vesicles (GUV) as cell models.[10]

The synergistic effect on membrane stability has been tracked back to an efficient regeneration of the carotenoid (Car) from the carotenoid radical cation ($Car^{\bullet+}$) as an initial oxidation product by the plant phenol (φ-OH)

$$Car^{\bullet+} + \varphi\text{-OH} \rightarrow Car + \varphi\text{-O}^{\bullet} + H^{+}$$

The bimolecular regeneration depends on the potential difference between the two redox couples, and moderately reducing phenols such as isoflavonoid daidzein result in the maximal rate close to the diffusion limit in agreement with the Marcus theory for electron transfer.[11] However, various bifunctional antioxidants that covalently link phenolic compounds to a carotenoid or a retinal analogue have been synthesized and studied in relation to their antioxidation activity recently. These bifunctional antioxidants could be categorized as two types, that is, with unconjugated linking[12−16] or with conjugated linking.[17−20] Some bifunctional antioxidants have been shown to outperform the antioxidative activity of the combination of the building blocks.[12,13,16,19,20] In the conjugated linking ones, which is so-called dyads, the bimolecular regeneration is replaced by intramolecular electron transfer between the carotenyl- and the flavonoid part of the dyad. Accordingly, it will be of interest to optimize such amphiphilic antioxidants with respect to radical scavenging efficiency by adjusting the length of linear conjugation. Reported are the synthesis of two new analogues of retinyldaidzein and all three dyads are compared with respect to radical scavenging together with their parent molecules. It is further investigated whether quantum mechanical calculations may assist in design of such amphiphilic dual-function antioxidants for the use in heterogenous foods.

Received: March 1, 2020
Accepted: May 18, 2020
Published: June 1, 2020

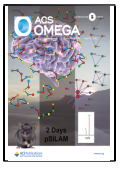

https://dx.doi.org/10.1021/acsomega.0c00925
ACS Omega 2020, 5, 13770−13776

Scheme 1. Molecular Structure of Retinal Homologues (R_6–R_{10}) and Retinylisoflavonoids (R_6-D–R_{10}-D)

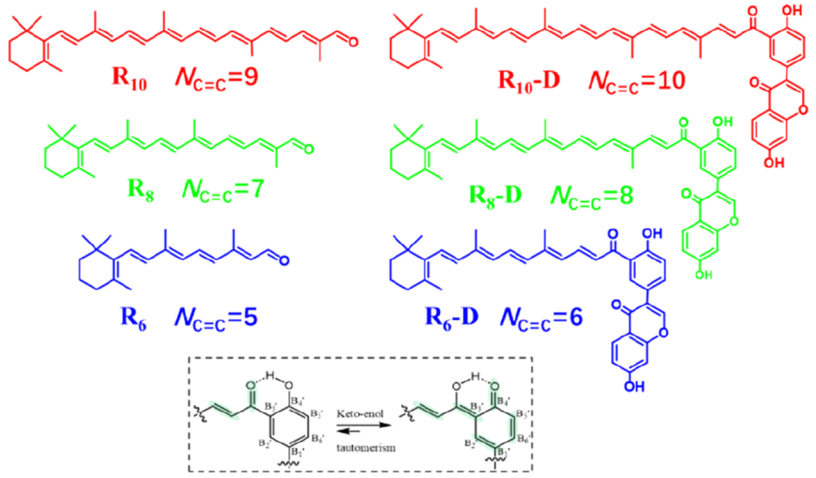

Table 1. Structural Comparison of Daidzein, R_6–R_8, and Dyads by Absorption Spectroscopy, ^{1}H NMR, and DFT Calculation

	conjugation length ($N_{C=C \text{ and } C=O}$)/keto	conjugation length ($N_{C=C \text{ and } C=O}$)/enol	energy (cm^{-1}) (λ_{max}, nm)/fwhm (cm^{-1})[a]	δ (B4′OH) (ppm)[b]	θ (0)[c]
daidzein				9.52	
R_6	6	6	26,247 (381)/5807		
R_8	8	8	23,474 (426)/5133		
R_{10}	10	10	21,692 (461)/4625		
R_6-D	7	10	22,472 (445)/5423	12.7349	0.15839
R_8-D	9	12	21,231 (471)/5702	12.7399	0.17523
R_{10}-D	11	14	20,243 (494)/6078	12.7901	0.17636

[a]fwhm: full width at half-maxima of the absorption band. [b]δ: (B4′-OH): chemical shift of B4′-OH by ^{1}H NMR. [c]θ: dihedral angle between B3′-B4′-OH and B3′-terminal carbonyl group of retinal analogues in dyads obtained by DFT calculation.

RESULTS AND DISCUSSION

From retinal (C22 with 6 conjugated double bonds, R_6), from the C27 homologue with 8 conjugated double bonds (R_8), and from the C32 homologue with 10 conjugated double bonds (R_{10}), each of the three dyads (R_6-D, R_8-D, and R_{10}-D) shown in Scheme 1, were synthesized. The two newly synthesized compounds, R_8-D and R_{10}-D, were characterized together with R_6-D as previously reported and tested for their radical scavenging efficiency using the semistable radicals $ABTS^{\bullet+}$ and $DPPH^{\bullet}$ together with the three homologue aldehydes, that is, R_6, R_8, and R_{10}.

Electronic Structures and Conjugation Length. As reported in our previous work,[20] based on ^{1}H NMR results (Table 1, see Supporting Information for NMR date), the chemical shift of B4′-OH in the three dyads downshifted from 9.52 to ~12.7 ppm in comparison with the chemical shift in daidzein. The intramolecular hydrogen bond between the bridge carbonyl group and B4′-OH phenol which stabilize the preferred flat conformation including the polyene backbone and ring B of daidzein has accordingly been adopted by the three retinylisoflavonoid dyads. The optimized conformation of all of the retinal homologues and dyads by density functional theory (DFT) calculations is shown in Figure S2. All three dyads take an "L" conformation. With the conjugation length increasing, the dihedral angle between polyene and the B ring of daidzein also increases (Table 1). Intramolecular hydrogen bond stabilizing this conformation also facilitates the keto–enol tautomerism equilibrium favoring the "enol" form in the dyads (as shown in Scheme 1), in agreement with the chemical shift of B4′-OH. These conclusions are further supported by the following spectral data.

Figure 1 shows the UV–visible absorption spectra of retinal homologues (R_6–R_{10}) and the corresponding retinylisoflavonoid dyads (R_6-D–R_{10}-D). Except for the absorption originated from daidzein in the UV region, the most intense absorption for all the compounds originates from the π–π^* transition of the conjugation backbone, which is red-shifted by

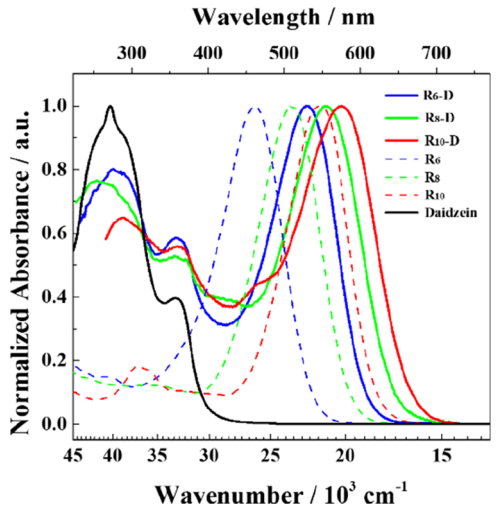

Figure 1. UV–visible absorption spectra of retinal homologues (R_6–R_{10}, dashed lines) and their conjugated dyads with daidzein (R_6-D–R_{10}-D, solid lines) in methanol.

https://dx.doi.org/10.1021/acsomega.0c00925
ACS Omega 2020, 5, 13770–13776

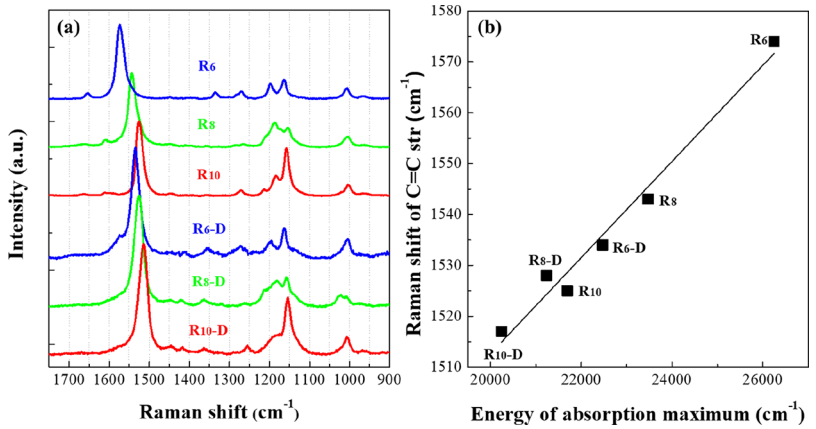

Figure 2. Raman spectra of retinal homologues ($\mathbf{R_6}$–$\mathbf{R_{10}}$) and dyads ($\mathbf{R_6}$-**D**–$\mathbf{R_{10}}$-**D**) (a) and the linear correlation of the Raman shift of the C=C stretching mode with energy of absorption maximum (b).

an increase of the conjugation length. The spectral red-shift obviously does not agree with that of the number of conjugated C=C bonds of the keto form but rather with the number of conjugated C=C bonds of the enol form as shown as column 1 and 2 (see Table 1), respectively. Although the conjugated C=C bond number of $\mathbf{R_{10}}$ is same with that of $\mathbf{R_6}$-**D** based on the "enol" structure as shown in Scheme 1 and summarized in Table 1, the absorption of $\mathbf{R_{10}}$ is more red-shifted because of the more cis character of the conjugated double bond in $\mathbf{R_6}$-**D** connecting to the daidzein which accordingly decreases the effective conjugation length.

Resonance Raman spectra of the three dyads and the three retinal homologues are shown in Figure 2a. Both the dyads and the aldehydes show a similar spectral pattern, which is characteristic for polyenes. DFT calculation results help to assign Raman lines, and the results are listed in Table S1. For the three aldehydes, the weak C=O stretching mode is seen at 1653–1666 cm^{-1}, and the frequency upshift increases as the conjugation length increases. For the three dyads, only for $\mathbf{R_6}$-**D** the Raman line, assigned as the C=O stretching mode coupled with the C=C stretching mode, could be seen at 1574 cm^{-1}. In the other two dyads, the C=O stretching mode was absent. The Raman shift of the C=C backbone stretching mode has an obvious dependence of the conjugation length as shown as Figure 2b, a phenomenon also reported for retinal derivatives and carotenoids.[21] These results further strengthen the enol form assignment for the dyads.

Conjugation Length and Radical Scavenging Efficiency. Oxidation potential is a most important factor in determining the radical scavenging capacity of antioxidants.[22] The oxidation potential of the three aldehydes and three dyads was measured in acetonitrile solution, and the results are summarized in Table 2. Except for $\mathbf{R_6}$, the other five compounds have lower oxidative potentials than daidzein. Notably, the dyads are more reducing than their parent aldehydes, although the potential difference decreases with increasing chain lengths.

The rate of scavenging of the lipophilic radical $DPPH^{\bullet}$ and the water-soluble radical $ABTS^{\bullet+}$ by the six target compounds was measured by a stopped-flow technique using visible spectroscopy, as shown in Figure 3. The initial rate of each reaction was used to describe the radical scavenging capability for each compound quantitatively, and the results are listed in Table 2 and converted to the second-order rate constants, as described in the Supporting Information.

Table 2. Oxidation Potential in Acetonitrile (V *vs* NHE) and Free Radical Scavenging Efficiency as the Second-Order Rate Constant for $\mathbf{R_6}$–$\mathbf{R_{10}}$ and Dyads in Homogeneous Solution

	oxidation potential (V)	$k_{DPPH^{\bullet}}$ ($mol^{-1}\cdot L\cdot min^{-1}$)[a]	$k_{ABTS^{\bullet+}}$ ($mol^{-1}\cdot L\cdot min^{-1}$)[b]
daidzein	1.217	2.40×10^2	18.86×10^4
$\mathbf{R_6}$	1.377[c]	1.21×10^2	3.88×10^4
$\mathbf{R_8}$	1.129	3.77×10^2	8.33×10^4
$\mathbf{R_{10}}$	0.966	4.23×10^2	12.82×10^4
$\mathbf{R_6}$-**D**	1.178	2.58×10^2	7.06×10^4
$\mathbf{R_8}$-**D**	1.035	5.06×10^2	10.85×10^4
$\mathbf{R_{10}}$-**D**	0.957	5.48×10^2	17.14×10^4

[a]Second-order rate constant from the initial rate of free radical scavenging in ethanol. [b]Second-order rate constant from the initial rate of free radical scavenging in 1:1 water–ethanol. [c]E^{o} = 1.377 V has been reported for acetonitrile as the solvent.[23]

In Figure 4 the correlation between the second-order rate constant and the oxidation potential is shown for $ABTS^{\bullet+}$ and $DPPH^{\bullet}$. In the water–ethanol solvent, the logarithm of the second-order rate constant for radical scavenging of $ABTS^{\bullet+}$ is seen to depend linearly on the potential of the radical scavenger, and the compound with longer conjugated carbon chains is the more reducing and faster reacting compound. The linear free energy relationship seen for $ABTS^{\bullet+}$ is less evident for $DPPH^{\bullet}$, although scavenging by daidzein now is covered by the linear relationship. For the $ABTS^{\bullet+}$ scavenging reaction, the driving force is concluded mainly to be determined by the redox potential difference between the reductant (antioxidants in this study) and the oxidant (free radical) suggesting bimolecular electron transfer as the rate-determining step. For the $DPPH^{\bullet}$ scavenging reaction, the mechanism is more complicated and a contribution from hydrogen atom transfer seems important as also proved by the slower rate for daidzein. The rate is faster for $ABTS^{\bullet+}$ than for $DPPH^{\bullet}$ as would be expected when comparing electron transfer with hydrogen atom transfer under similar conditions. The role of hydrogen atom transfer finds some support by the linear free energy relationship observed between the bond dissociation energy (BDE) for the O–H bond of 7-OH of daidzein (but not of 4′-OH), and the rate of reaction of the three dyads with $DPPH^{\bullet}$ is as discussed below.

https://dx.doi.org/10.1021/acsomega.0c00925
ACS Omega 2020, 5, 13770–13776

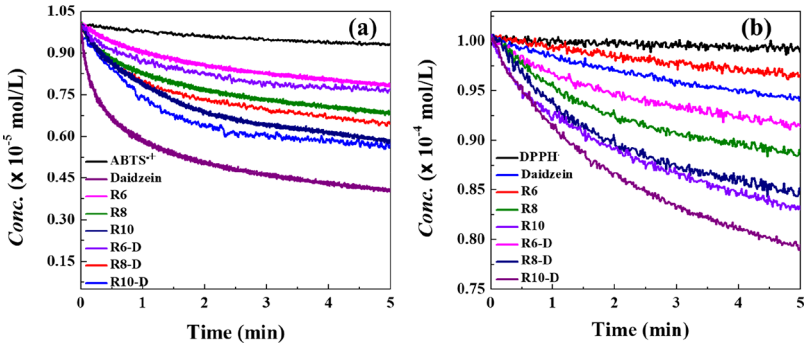

Figure 3. Absorbance change during ABTS$^{\bullet+}$ (a) and DPPH$^{\bullet}$ (b) scavenging in 1:1 water ethanol and ethanol, respectively, at 25 °C.

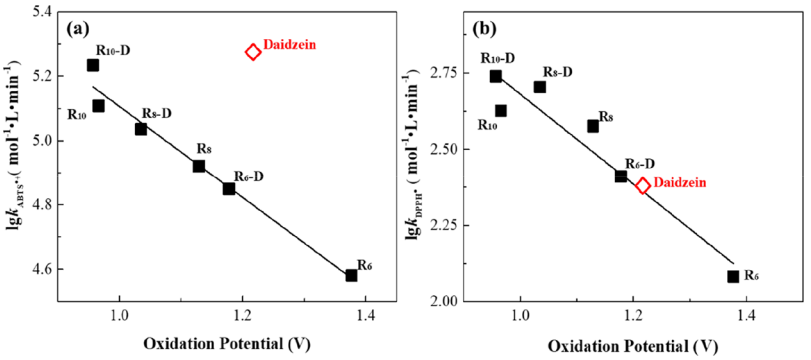

Figure 4. Dependence on their oxidation potentials of the second-order rate constant (k) for scavenging of ABTS$^{\bullet+}$ in 1:1 water ethanol (a) and DPPH$^{\bullet}$ in ethanol (b) at 25 °C by the retinal analogues and the daidzein conjugates.

Table 3. Calculated PDE, IP, and BDE of Daidzein, R_6−R_{10}, and Dyads[a]

compound		daidzein	R_6	R_8	R_{10}	R_6-D	R_8-D	R_{10}-D
PDE (kcal·mol^{-1})	A7-OH/A7-O$^-$	328.18				326.12	325.86	325.71
	B4′-OH/B4′-O$^-$	339.53				345.05	344.87	344.77
BDE (kcal·mol^{-1})	A7-OH/A7-O$^{\bullet}$	85.19				85.45	85.42	85.38
	B4′-OH/B4′-O$^{\bullet}$	80.93				95.84	95.82	95.86
IP (kcal·mol^{-1})		633.06	623.57	611.38	603.06	612.40	604.75	599.72
Log P		2.73	4.86	6.31	7.60	8.70	10.00	11.30
dipole moment (debye)		3.03	6.35	7.27	8.22	8.35	8.79	9.26
polarizability (α)		175.52	315.88	511.38	757.99	645.26	897.06	1190.05

[a]Quantum chemical results: PDE, proton dissociation energy; BDE, bond dissociation energy; IP, ionization potential was from DFT calculation, while Log P was obtained from MarvinSketch V6.14.

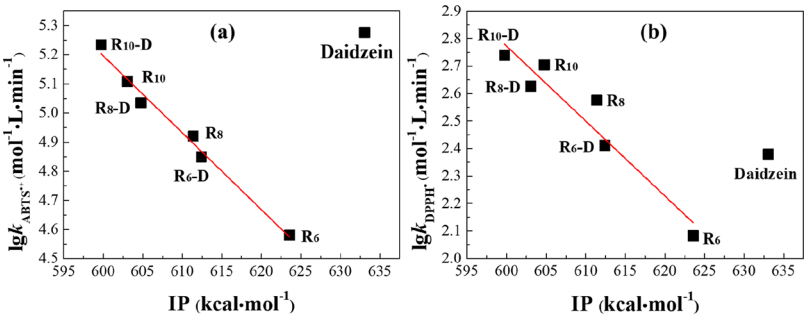

Figure 5. Correlation of lg k (k is the second-order rate constant of the initial rate for radical scavenging kinetics) with IP of antioxidants for ABTS$^{\bullet+}$ (a) and DPPH$^{\bullet}$ (b).

A series of physicochemical parameters calculated by DFT are summarized in Table 3 for the potential antioxidants. Ionization potential (IP) indicating the capability of one-electron donation of antioxidants in the gas phase is linearly correlated with the oxidation potential of the six antioxidants not including daidzein. IP is accordingly expected to have a similar correlation with lg k as with the oxidation potential as confirmed in Figure 5a,b. Figure 6a,b indicates a linear dependence of the conjugation length (represented by energy of the absorption maxima) in each series of homologues and

https://dx.doi.org/10.1021/acsomega.0c00925
ACS Omega 2020, 5, 13770−13776

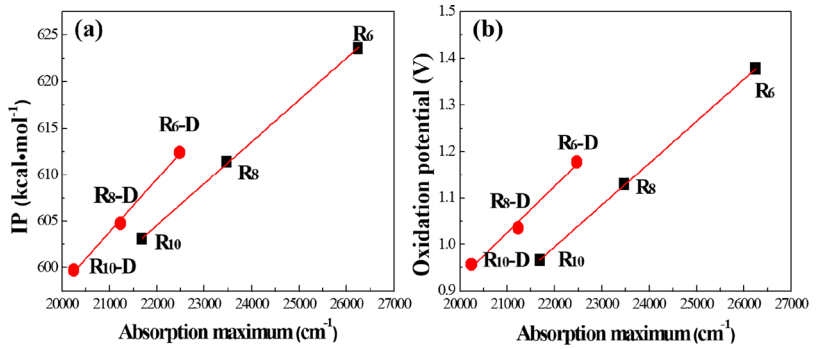

Figure 6. Correlation of IP (a) and oxidative potential (b) of antioxidants with the electronic transition energy of absorption maximum.

the oxidation potential and IP. However, the linear free-energy relationship differs between the two series of compounds, which could be explained as follows: the one-electron donation capability is not only determined by the conjugation length but is also determined by the structure of groups from which electrons are donated. Notably, the terminal group of retinal homologues is an aldehyde, while that of the dyads include a phenol or an enol group. Other correlations between spectral data and IP, proton dissociation enthalpy (PDE), BDE, and rate of radical scavenging are shown in the Supporting Information.

The linear free-energy relationship seen for the scavenging of the $ABTS^{\bullet+}$ radical has a slope of -1.37 ± 0.01 (Figure 4a) and notably almost the same slope is seen with a value of -1.47 ± 0.22 for the scavenging of $DPPH^{\bullet}$ by the same series of scavengers (Figure 4b). This similarity confirms a similar mechanism despite the rather large difference in rate constants by more than a factor of 100 with $ABTS^{\bullet+}$ being the more reactive.

It should also be noted that a $DPPH^{\bullet}$ scavenging reaction mainly involving the daidzein A7-OH and B4′-OH groups can only occur through proton transfer through the preferential enol form. In contrast, the A7-OH group could also be involved in the reaction through both proton transfer and hydrogen atom transfer, which is equal to proton transfer followed by electron transfer.

Antioxidant synergism is characteristic for the combination of moderately reducing (iso)flavonoids and carotenoids for protection of heterogeneous foods and biological membranes in general.[4] Covalently linking an isoflavonoid such as daidzein to a retinal homologue is known to increase this synergism in antioxidant efficiency as the formed dyad is oriented in the water−lipid interface with the conjugated carbon chain penetrating the lipid phase, and the isoflavonoid is providing contact to the aqueous phase.[19,20] An increasing length of the conjugated chain makes the dyad more reducing but still with the characteristic "L"-shape through keto−enol tautomerism in effect increasing the radical scavenging efficiency as is demonstrated in the present study. From the linear free-energy relationship between the electron donation rate and oxidation potential radical scavenging efficiency may be predicted for this type of compounds from their UV−vis absorption spectra because both the oxidation potential and the IP have been found to depend linearly on the energy of the $\pi-\pi^*$ transition as may be estimated by the position of the absorption maximum.

CONCLUSIONS

Radical scavenging efficiency can be predicted from visible absorption spectra for retinal (C20) and the C25 and C30 homologues and their dyads (conjugates) obtained by covalently linking C22, C27, and C32 homologues of retinal with the isoflavonoid daidzein as was demonstrated with the perspective of rational design of bifunctional amphiphilic antioxidants with potential as drugs or as use for food protection. Oxidation potentials as determined by cyclic voltammetry and IPs based on quantum mechanical calculations for the aldehydes and the dyads were demonstrated to decrease linearly with the wavenumber for the absorption maximum. The logarithm of the second-order rate constant for scavenging of $ABTS^{\bullet+}$ increased linearly with decreasing oxidation potential suggestion that longer conjugation in the antioxidant increases the rate of electron transfer. A similar linear free-energy relationship was found for the rate of scavenging the DPPH neutral radical, also including daidzein, which may indicate involvement of hydrogen atom transfer from an isoflavonoid phenol groups.

MATERIALS AND METHODS

Daidzein was from Huike Plant Exploitation Inc. (>98%, Shanxi, China). 2,2′-Azinobis(3-ethylbenzothiazoline-6-sulfonic acid) (ABTS), potassium *tert*-butoxide, retinol acetate (>99%), aluminum chloride, acetic anhydride, and manganese dioxide were from Innochem (Beijing, China). 2,2-Diphenyl-1-picrylhydrazyl (DPPH) was from Alladdin (Shanghai, China). *trans*-β-Apo-8′-carotenal ($\mathbf{R_{10}}$, 4 of Scheme S1) was from Shanghai Yuanye Bio-Technology Co., Ltd (≥96%, Shanghai, China). All other reagents and solvents were supplied by Beijing Tongguang Fine Chemicals Company (>99%, Beijing, China) and used as received without further purification except where noted. Retinal ($\mathbf{R_6}$, 1 of Scheme S1) and 3′-acetyldaidzein (7 of Scheme S1) were synthesized following the published procedure.[20]

The synthetic route is shown in Scheme S1 in the Supporting Information and briefly described as follows.

12′-Apo-β-carotenal (3). C5P phosphonium salt (**2**) (2.1754 g, 5.06 mol) was dissolved in 15 mL of dry CH_3OH under argon for 0.5 h. Retinal ($\mathbf{R_6}$, **1**) (0.0939 g, 0.33 mol) in dry CH_2Cl_2 was added in drops and stirred at 40 °C for 1 h. Mixtures of reaction were quenched by adding 1 mL of water, and CH_3OH was removed under reduced pressure. The aqueous layer was extracted four times with 30 mL of dichloromethane. The combined organic phase was dried by anhydrous $MgSO_4$, filtered, and concentrated. The crude product was treated with *p*-toluenesulfonic acid (40 mg) in 30

https://dx.doi.org/10.1021/acsomega.0c00925
ACS Omega 2020, 5, 13770−13776

mL of dichloromethane for 4 h. Then, the solution was washed twice with 30 mL of $NaHCO_3$ diluted aqueous solution followed by 30 mL of water. The combined organic phase was dried over anhydrous Na_2SO_4, filtrated, and concentrated under reduced pressure. The crude product was purified by silica gel column chromatography (eluted with diethyl ether and light petroleum) to afford 100 mg of red oil (0.29 mmol, 87%).[24]

3′(14′-Apo-β-carotene-14′-carbonyl)-daidzein (**8**) was synthesized as previously described.[20] The yield was 23%.

3′(10′-Apo-β-carotene-10′-carbonyl)-daidzein (**9**). 3′-Acetyldaidzein (**7**) (1.2 g, 0.0042 mol), potassium *tert*-butoxide (1.00 g, 0.0089 mol), and 100 mL of anhydrous ethanol were kept stirring in a round-bottomed flask under the protection of a nitrogen atmosphere. 12′-Apo-β-carotenal (**3**) (0.7357 g, 0.0021 mol) was added to the mixture and kept refluxing at 100 °C for 3 h. The mixture was cooled down to room temperature and poured into 40 mL of stirred water, and then, the pH was adjusted to 4−5. After extracting with ethyl acetate (3 × 50 mL), the combined organic phase was dried and evaporated to dryness and then purified by silica gel column chromatography (eluted with cyclohexane and tetrahydrofuran) to give $\mathbf{R_8}$-**D** with a yield of 17%.

3′(6′-Apo-β-carotene-6′-carbonyl)-daidzein (10). Using the same procedure as for synthesis of compound **9**, compound **10** in Scheme 1, that is, $\mathbf{R_{10}}$-**D**, was synthesized from 3′-acetyldaidzein (**7**) and 8′-apo-β-carotenal (**4**) with a yield of 14%.[20]

All the structural characterization data is listed in the Supporting Information in the Section 1 "Structural Characterization of Target Compounds".

Spectroscopic Characterization. ^1H and ^{13}C NMR spectra were obtained on a Bruker AM 400 or 500 MHz spectrometer (Karlsruhe, Germany). HRMS data were obtained by ESI ionization from a Thermo Scientific Q Exactive HF (Waltham, MA, USA). UV−visible absorption spectra in methanol were obtained on an absorption spectrometer (Cary 50, Varian, Australia). Raman spectra were recorded on a Raman spectrometer (XploRA PLUS, Horiba Scientific Ltd., France) under excitation at 532 nm.

Determination of Oxidation Potentials. For cyclic voltammetric measurements, anhydrous acetonitrile solutions with a concentration of 1.0×10^{-5} M were prepared under the protection of dried N_2, and the final concentration of the supporting electrolyte, tetra-*n*-butylammonium perchlorate (TBAP), was 0.10 M. Each solution was prepared directly into an electrochemical cell equipped with the standard three electrodes, that is, a glassy carbon working electrode, a Pt wire counter electrode, and a silver wire pseudoreference electrode calibrated against the ferrocene/ferrocenium couple. The electrochemical cell was sealed inside the glove box to maintain a nitrogen atmosphere and then subjected to cyclic voltammetry measurement on a CHI 760D electrochemical analyzer (ChenHua Instruments Inc., Shanghai, China). All of the measurements were done at room temperature (25 ± 1 °C) and reported *versus* the NHE.

DPPH• and ABTS•+ Scavenging Kinetics. Kinetics of scavenging of the semistable free radicals (DPPH• and $ABTS^{\bullet+}$) by the potential antioxidants were determined by stopped-flow technique performed on a RX2000 Rapid-Mixing Stopped-Flow Unit (Applied Photophysics Ltd., Surrey, United Kingdom). To avoid the interference from spectral overlap, the probing wavelength of DPPH• was set at 700 nm instead of at the absorption maximum at 516 nm. The probing wavelength of $ABTS^{\bullet+}$ was set at 734 nm. The DPPH• solution was prepared in ethanol (2.0×10^{-4} M) and the $ABTS^{\bullet+}$ was prepared in the water−ethanol 1:1 mixture (2.0×10^{-5} M). The solutions of antioxidants in ethanol were mixed with free radical solutions in a volume ratio of 1:1. Second-order rate constants were calculated from initial change in absorption, see Supporting Information.

Theoretical Calculations. The molecular geometries of retinal and retinylisoflavonoid homologues and their deprotonated and oxidized forms were optimized with the UB3LYP DFT in conjunction with the 6-31G(d,p) basis set for BDE and IP and the 6−31 +G(d,p) basis set for PDE by the use of the Gaussian 09 package. The gas-phase PDE, BDE, and IP were derived as the enthalpy differences of the reactions ArOH → ArO^- + H^+, ArOH → ArO• + H•, and ArOH → $ArOH^{\bullet+}$ + e, respectively. The calculated dipole moment, polarizability (α), and Raman spectra of all the studied compounds were based on the 6-31G(d,p) basis set. The bandwidths of Raman lines were set to 4 cm^{-1} (fwhm, full width at half-maximum).[25,26] The calculation of Log_{10} partition (Log *P*) of the compounds was performed by MarvinSketch V6.14 (ChemAxon, 2018).

■ ASSOCIATED CONTENT

Supporting Information

The Supporting Information is available free of charge at https://pubs.acs.org/doi/10.1021/acsomega.0c00925.

Synthetic protocols of 3′(10′-Apo-β-carotene-10′-carbonyl)-daidzein ($\mathbf{R_8}$-**D**) and 3′(6′-Apo-β-carotene-6′-carbonyl)-daidzein ($\mathbf{R_{10}}$-**D**); second-order rate constant calculation; optimized molecular geometry; cyclic voltammetry; correlation between DFT and experimental results; assignment of Raman lines by DFT calculation; cartesian coordinates of the optimized geometries; ADME properties calculation (PDF)

■ AUTHOR INFORMATION

Corresponding Author

Peng Wang − *Department of Chemistry, Renmin University of China, Beijing 100872, China;* orcid.org/0000-0001-7019-9885; Phone: +86-10-62516604; Email: wpeng@iccas.ac.cn

Authors

Yang-Lin Jiang − *Department of Chemistry, Renmin University of China, Beijing 100872, China*

Bai-Ling Chen − *Department of Chemistry, Renmin University of China, Beijing 100872, China*

Xiao-Kun Yan − *Department of Chemistry, Renmin University of China, Beijing 100872, China*

Yi Xu − *Department of Chemistry, Renmin University of China, Beijing 100872, China;* orcid.org/0000-0003-4723-6312

Chen-Chen Zhao − *Department of Chemistry, Renmin University of China, Beijing 100872, China*

Zi-Li Chen − *Department of Chemistry, Renmin University of China, Beijing 100872, China;* orcid.org/0000-0002-0473-6395

Jian-Ping Zhang − *Department of Chemistry, Renmin University of China, Beijing 100872, China;* orcid.org/0000-0002-9216-2386

Leif H. Skibsted − *Department of Food Science, University of Copenhagen, Frederiksberg 1958, Denmark;* orcid.org/0000-0003-1734-5016

Complete contact information is available at: https://pubs.acs.org/10.1021/acsomega.0c00925

Notes

The authors declare no competing financial interest.

■ ACKNOWLEDGMENTS

This work has been supported by the Natural Science Foundation of China (21673289, 21273282, 21673288, and 21173265).

■ ABBREVIATIONS

GUV, giant unilamellar vesicles; Car, carotenoid; $Car^{\bullet+}$, carotenoid radical cation; ABTS, 2,2′-azinobis(3-ethylbenzothiazoline-6-sulfonic acid); DPPH, 2,2-diphenyl-1-picrylhydrazyl; $\mathbf{R_6}$ (C20), retinal; $\mathbf{R_8}$ (C25), 12′-apo-β-carotenal; $\mathbf{R_{10}}$ (C30), *trans*-β-apo-8′-carotenal; $\mathbf{R_6}$**-D** (C22), 3′(14′-apo-β-carotene-14′-carbonyl)-daidzein; $\mathbf{R_8}$**-D** (C27), 3′(10′-apo-β-carotene-10′-carbonyl)-daidzein; $\mathbf{R_{10}}$**-D** (C32), 3′(6′-apo-β-carotene-6′-carbonyl)-daidzein; DFT, density functional theory; PDE, proton dissociation enthalpy; BDE, bond dissociation energy; IP, ionization potential

■ REFERENCES

(1) Liang, J.; Tian, Y.-X.; Yang, F.; Zhang, J.-P.; Skibsted, L. H. Antioxidant synergism between carotenoids in membranes. Astaxanthin as a radical transfer bridge. *Food Chem.* **2009**, *115*, 1437−1442.

(2) Rodriguez-Amaya, D. B. Status of carotenoid analytical methods and in vitro assays for the assessment of food quality and health effects. *Curr. Opin. Food Sci.* **2015**, *1*, 56−63.

(3) Galano, A. Relative antioxidant efficiency of a large series of carotenoids in terms of one electron transfer reactions. *J. Phys. Chem. B* **2007**, *111*, 12898−12908.

(4) Burke, M.; Edge, R.; Land, E. J.; McGarvey, D. J.; Truscott, T. G. One-electron reduction potentials of dietary carotenoid radical cations in aqueous micellar environments. *FEBS Lett.* **2001**, *500*, 132−136.

(5) Tian, Y.-X.; Han, R.-M.; Zhang, J.-P.; Skibsted, L. H. Effect of polar solvents on β-carotene radical precursor. *Free Radical Res.* **2008**, *42*, 281−286.

(6) Naczk, M.; Shahidi, F. Extraction and analysis of phenolics in food. *J. Chromatogr. A* **2004**, *1054*, 95−111.

(7) Madhujith, T.; Naczk, M.; Shahidi, F. Antioxidant activity of common beans (phaseoul vulgaris l). *J. Food Lipids* **2005**, *11*, 220−233.

(8) Shahidi, F.; Chavan, U. D.; Naczk, M.; Amarowicz, R. Nutrient distribution and phenolic antioxidants in air-classified fractions of beach pea (lathyrus maritimus l.). *J. Agric. Food Chem.* **2001**, *49*, 926−933.

(9) Naczk, M.; Pegg, R. B.; Zadernowski, R.; Shahidi, F. Radical scavenging activity of canola hull phenolics. *J. Am. Oil Chem. Soc.* **2005**, *82*, 255−260.

(10) Liu, X.-C.; Du, H.-H.; Fu, L.-M.; Han, R.-M.; Wang, P.; Ai, X.-C.; Zhang, J.-P.; Skibsted, L. H. Integrity of membrane structures in giant unilamellar vesicles as assay for antioxidants and prooxidants. *Anal. Chem.* **2018**, *90*, 2126−2133.

(11) Marcus, R. A. Electron transfer reactions in chemistry: theory and experiment. *J. Electroanal. Chem.* **1993**, *32*, 1111−1121.

(12) Papa, T. B. R.; Pinho, V. D.; Nascimento, E. S. P. D.; Santos, W. G.; Burtoloso, A. C. B.; Skibsted, L. H.; Cardoso, D. R. Astaxanthin diferulate as a bifunctional antioxidant. *Free Radical Res.* **2014**, *49*, 102−111.

(13) Chambers, C. S.; Biedermann, D.; Valentová, K.; Petrásková, L.; Viktorová, J.; Kuzma, M.; Křen, V. Preparation of retinoyl-flavonolignan hybrids and their antioxidant properties. *Antioxidants* **2019**, *8*, 236−248.

(14) Hu, F.; Bu, Y. Z.; Liang, R.; Duan, R. M.; Wang, S.; Han, R. M.; Wang, P.; Ai, X. C.; Zhang, J. P.; Skibsted, L. H. Quercetin and daidzein β-apo-14'-carotenoic acid esters as membrane antioxidants. *Free Radical Res. Commun.* **2013**, *47*, 413−421.

(15) Larsen, E.; Abendroth, J.; Partali, V.; Schulz, B.; Sliwka, H.-R.; Quartey, E. G. K. Combination of vitamin E with a carotenoid: α-tocopherol and trolox linked to β-apo-8'-carotenoic acid. *Chem.—Eur. J.* **1998**, *4*, 113−117.

(16) Karagiannidou, E.; Storseth, T. R.; Sliwka, H.-R.; Partali, V.; Malterud, K. E.; Tsimidou, M. Synthesis of two modified carotenoids and their behavior during light exposure. *Eur. J. Lipid Sci. Technol.* **2003**, *105*, 419−426.

(17) Springer, J. W.; Taniguchi, M.; Krayer, M.; Ruzié, C.; Diers, J. R.; Niedzwiedzki, D. M.; Bocian, D. F.; Lindsey, J. S.; Holten, D. Photophysical properties and electronic structure of retinylidene−chlorin−chalcones and analogues. *Photochem. Photobiol. Sci.* **2014**, *13*, 634−650.

(18) Hundsdörfer, C.; Stahl, W.; Müller, T. J. J.; De Spirt, S. UVA photoprotective properties of an artificial carotenylflavonoid hybrid molecule. *Chem. Res. Toxicol.* **2012**, *25*, 1692−1698.

(19) Beutner, S.; Frixel, S.; Ernst, H.; Hoffmann, T.; Hernandez-Blanco, I.; Hundsdoerfer, C.; Kiesendahl, N.; Kock, S.; Martin, H.-D.; Mayer, B.; Noack, P.; Perez-Galvez, A.; Kock, G.; Scherrers, R.; Schrader, W.; Sell, S.; Stahl, W. Carotenylflavonoids, a novel group of potent, dual-functional antioxidants. *ARKIVOC* **2007**, *VIII*, 279−295.

(20) An, C.-B.; Liang, R.; Ma, X.-H.; Fu, L.-M.; Zhang, J.-P.; Wang, P.; Han, R.-M.; Ai, X.-C.; Skibsted, L. H. Retinylisoflavonoid as a novel membrane antioxidant. *J. Phys. Chem. B* **2010**, *114*, 13904−13910.

(21) Mukai, Y.; Koyama, Y.; Ito, M.; Tsukida, K. Raman spectra of cis-trans isomers of retinal homologues. key bands of unmethylated cis configurations and of all-trans parts of mono-cis isomers. *J. Raman Spectrosc.* **1986**, *17*, 387−396.

(22) Lien, E. J.; Ren, S.; Bui, H.-H.; Wang, R. Quantitative structure-activity relationship analysis of phenolic antioxidants. *Free Radical Biol. Med.* **1999**, *26*, 285−294.

(23) Tan, Y. S.; Urbančok, D.; Webster, R. D. Contrasting voltammetric behavior of different forms of vitamin a in aprotic organic solvents. *J. Phys. Chem. B* **2014**, *118*, 8591−8600.

(24) Ehlers, F.; Scholz, M.; Schimpfhauser, J.; Bienert, J.; Oum, K.; Lenzer, T. Collisional relaxation of apocarotenals: identifying the S* state with vibrationally excited molecules in the ground electronic state S_0*. *Phys. Chem. Chem. Phys.* **2015**, *17*, 10478.

(25) Xu, Y.; Qian, L.-L.; Yang, J.; Han, R.-M.; Zhang, J.-P.; Skibsted, L. H. Kaempferol binding to zinc(ii). efficient radical scavenging through increased phenol acidity. *J. Phys. Chem. B* **2018**, *122*, 10108−10117.

(26) Frisch, M. J.; Trucks, G. W.; Schlegel, H. B.; Scuseria, G. E.; Robb, M. A.; Cheeseman, J. R.; Scalmani, G.; Barone, V.; Mennucci, B.; Petersson, G. A.; Nakatsuji, H.; Caricato, M.; Li, X.; Hratchian, H. P.; Izmaylov, A. F.; Bloino, J.; Zheng, G.; Sonnenberg, J. L.; Hada, M.; Ehara, M.; Toyota, K.; Fukuda, R.; Hasegawa, J.; Ishida, M.; Nakajima, T.; Honda, Y.; Kitao, O.; Nakai, H.; Vreven, T.; Montgomery, J. A., Jr.; Peralta, J. E.; Ogliaro, F.; Bearpark, M.; Heyd, J. J.; Brothers, E.; Kudin, K. N.; Staroverov, V. N.; Kobayashi, R.; Normand, J.; Raghavachari, K.; Rendell, A.; Burant, J. C.; Iyengar, S. S.; Tomasi, J.; Cossi, M.; Rega, N.; Millam, J. M.; Klene, M.; Knox, J. E.; Cross, J. B.; Bakken, V.; Adamo, C.; Jaramillo, J.; Gomperts, R.; Stratmann, R. E.; Yazyev, O.; Austin, A. J.; Cammi, R.; Pomelli, C.; Ochterski, J. W.; Martin, R. L.; Morokuma, K.; Zakrzewski, V. G.; Voth, G. A.; Salvador, P.; Dannenberg, J. J.; Dapprich, S.; Daniels, A. D.; Farkas, Ö.; Foresman, J. B.; Ortiz, J. V.; Cioslowski, J.; Fox, D. J. *Gaussian 09*, Revision C.01; Gaussian Inc., **1994**.